

# The Pomeron, Odderon, and $N^*$ resonances in $\phi(1020)$ photoproduction

Sang-Ho Kim ( 金相鎬 )

Pukyong National University (PKNU)



Contents based on  
arXiv: 1904.05133 [hep-ph]

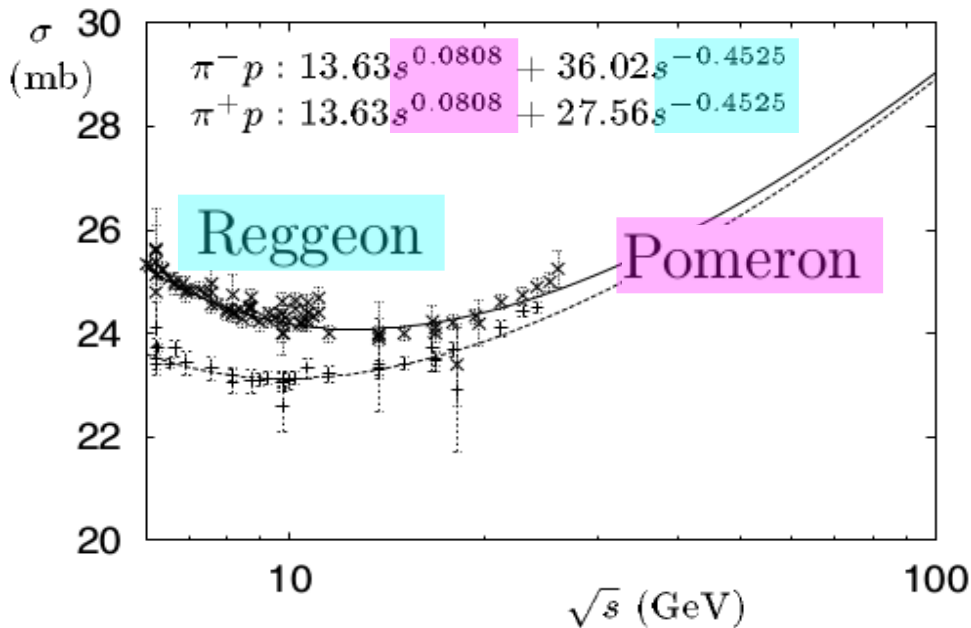
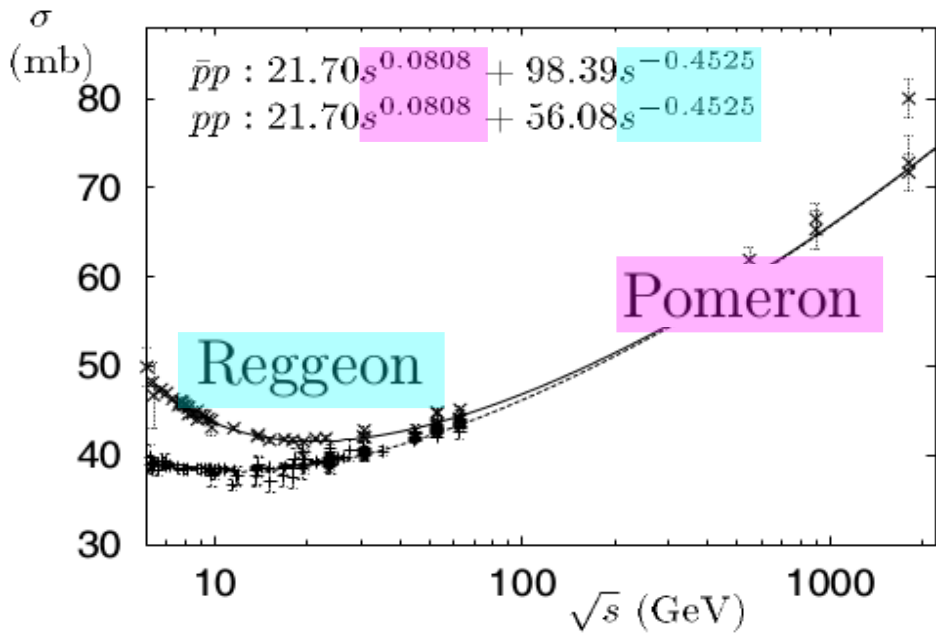
In collaboration with  
Seung-il Nam (PKNU)

# Contents

$$\gamma p \rightarrow \phi p$$

- ◆ Background
- ◆ Formalism
- ◆ Numerical Results
- ◆ Summary

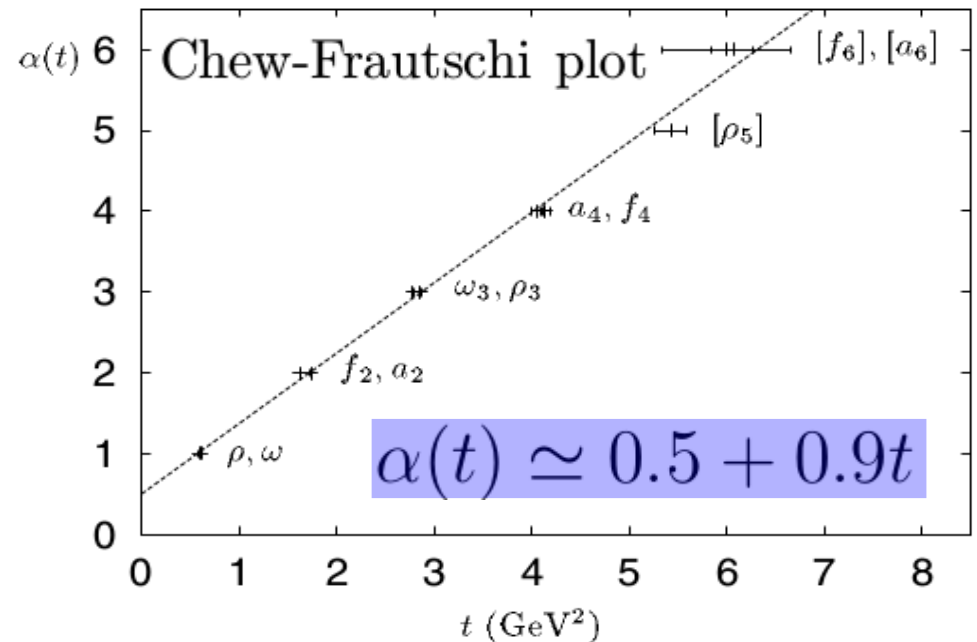
# Background



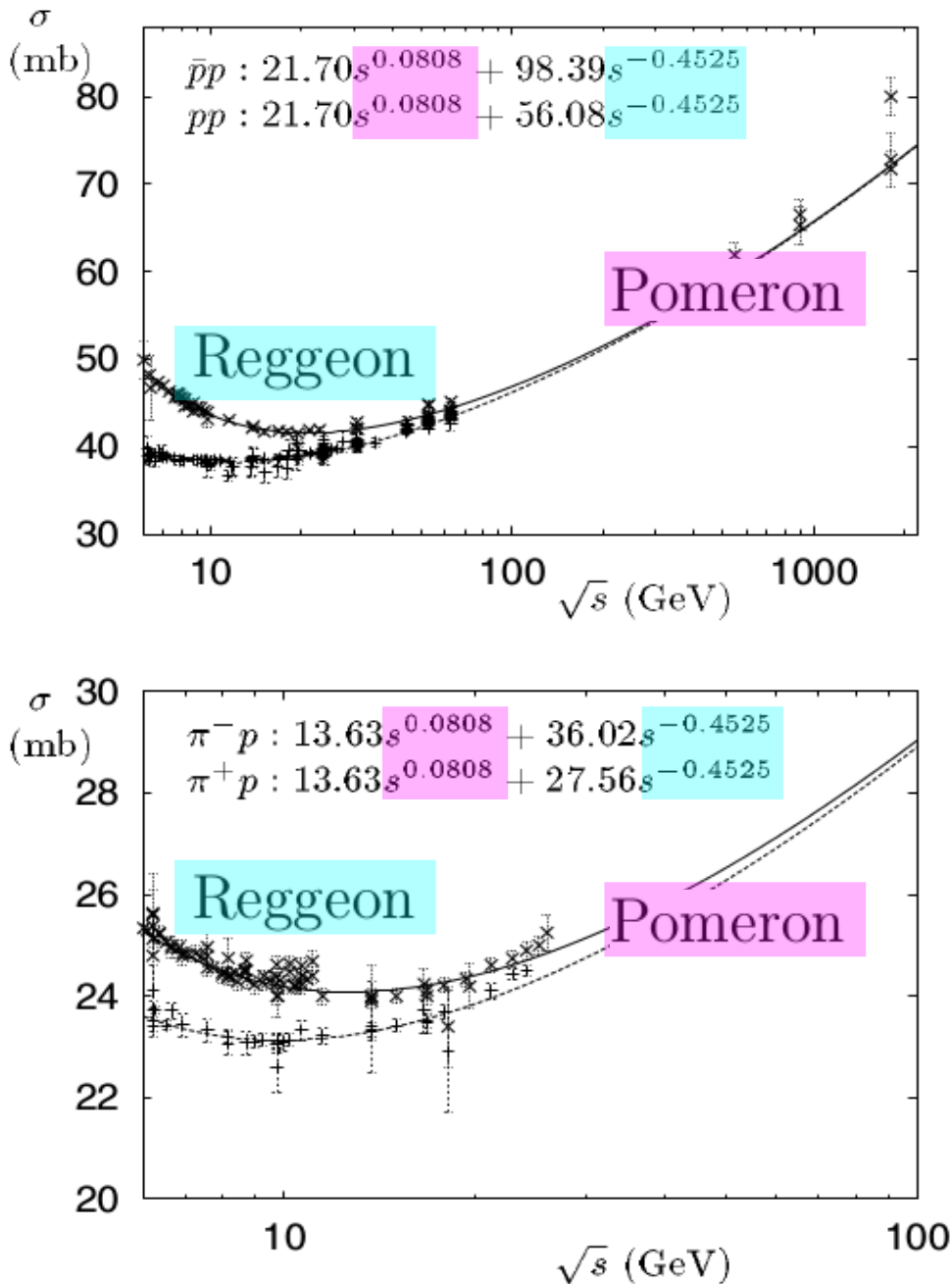
Donnachie, Pomeron Physics and QCD (2002)

## Reggeon (Meson exchange)

- Describes an exchange of a family of ordinary mesons.
- Governs relatively low energy regions.
- $(\rho, \omega)$  trajectories (C=-1, natural parity) &  $(f_2, a_2)$  trajectories (C=+1, natural parity) are all degenerate.



$$\sigma \propto s^{\alpha(0)-1} = s^{-0.5}$$



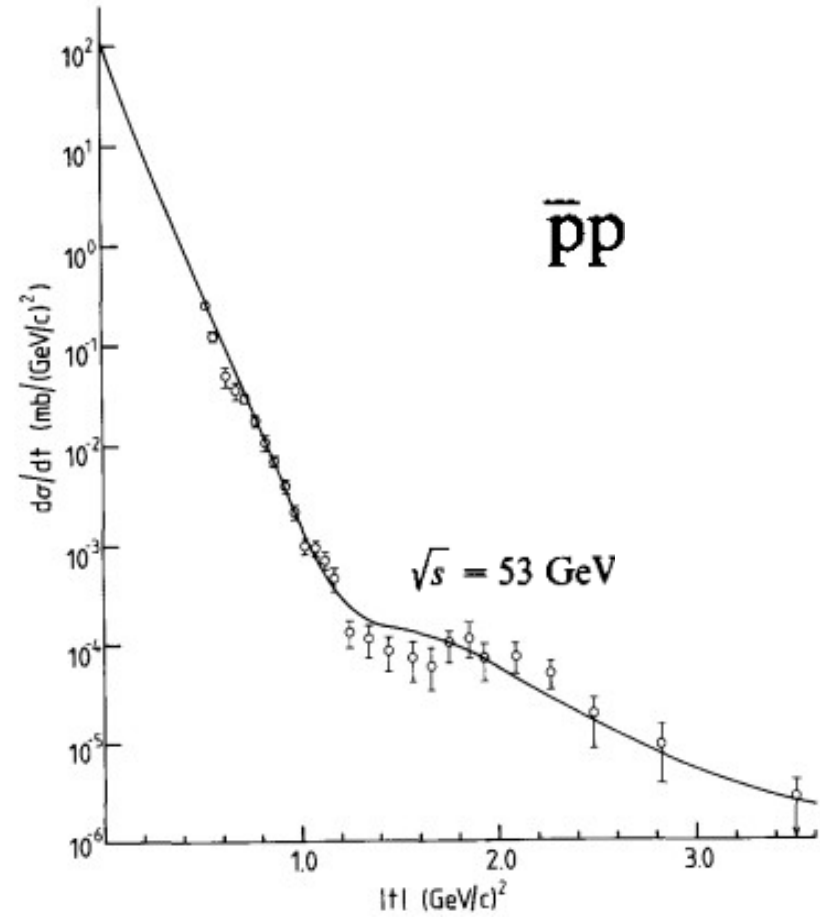
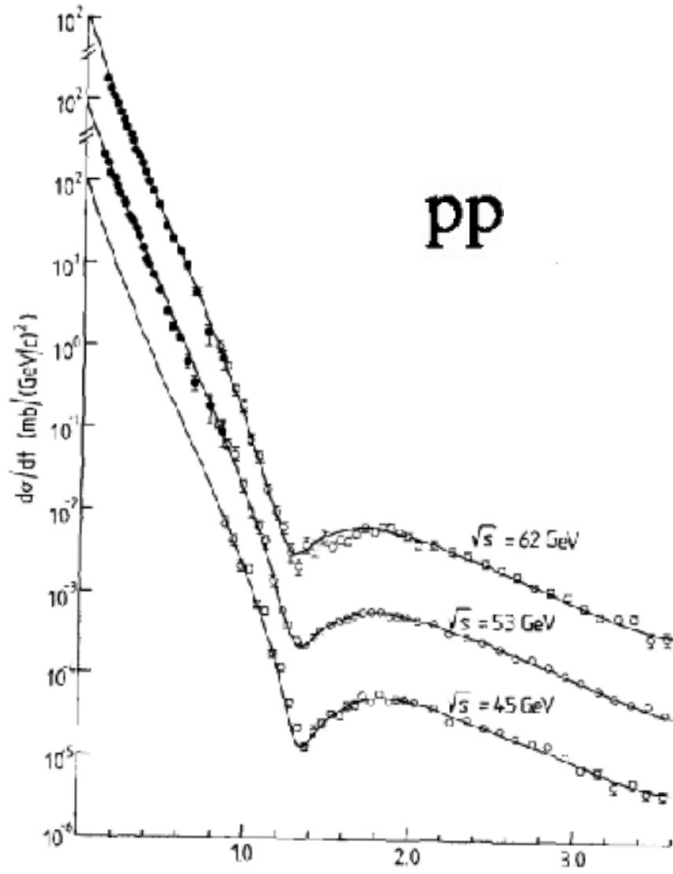
Donnachie, Pomeron Physics and QCD (2002)

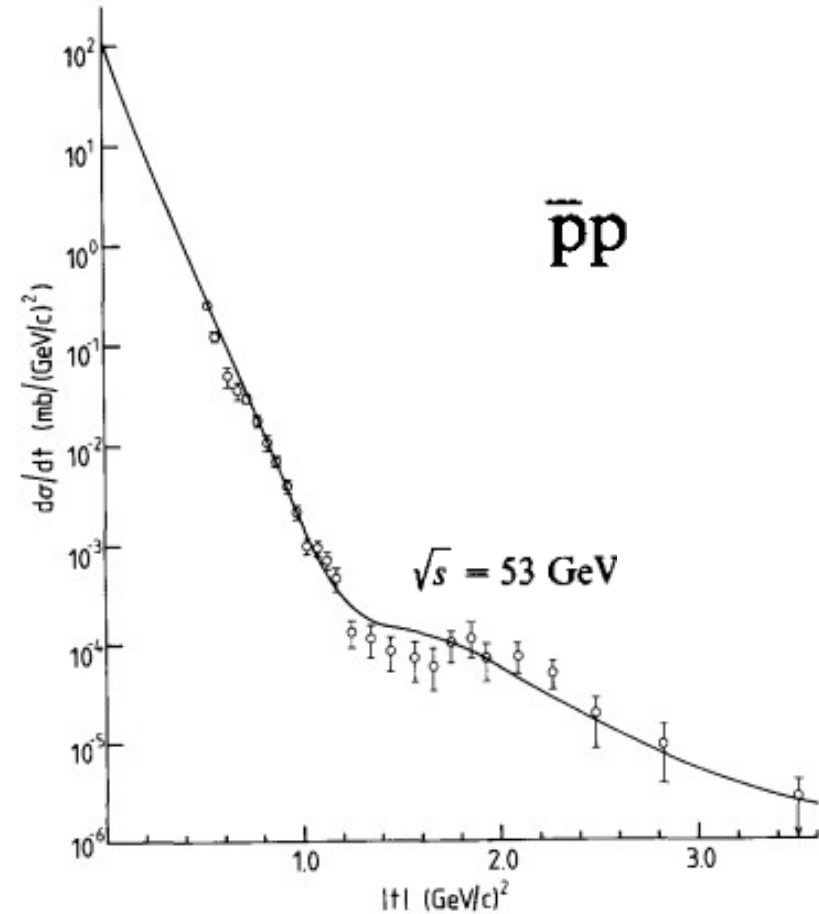
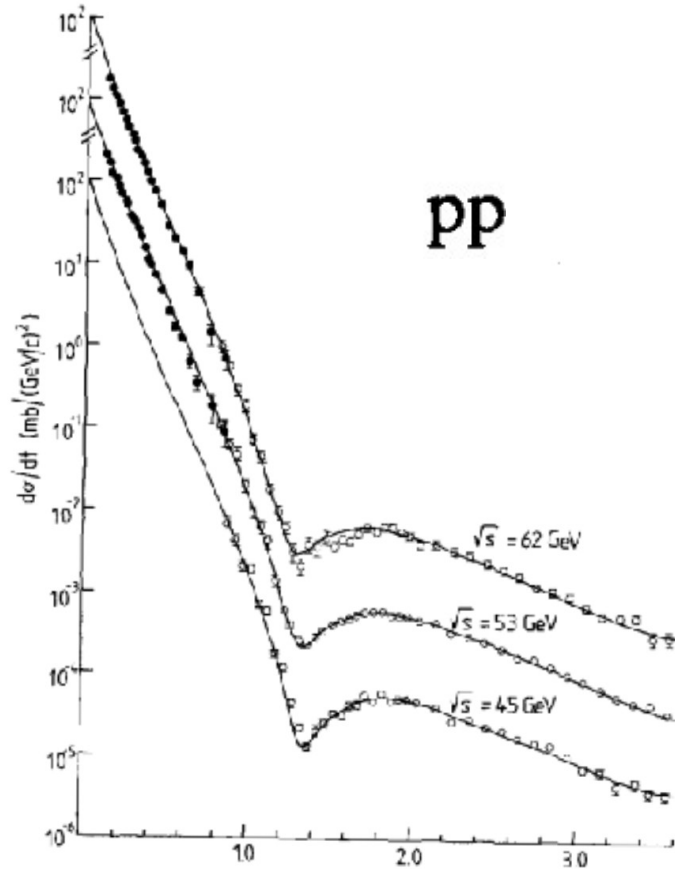
## Pomeron

- Is not associated with meson trajectories.
  - Is known as a gluon-rich Regge trajectory with vacuum quan. number, ( $J^{PC} = 0^{++}$ ).
  - Governs relatively high energy regions.
- 
- There is no deep theory reason for the Pomeron hypothesis, but the phenomenology based on which turns out to be very successful.
  - Pomeron trajectory:

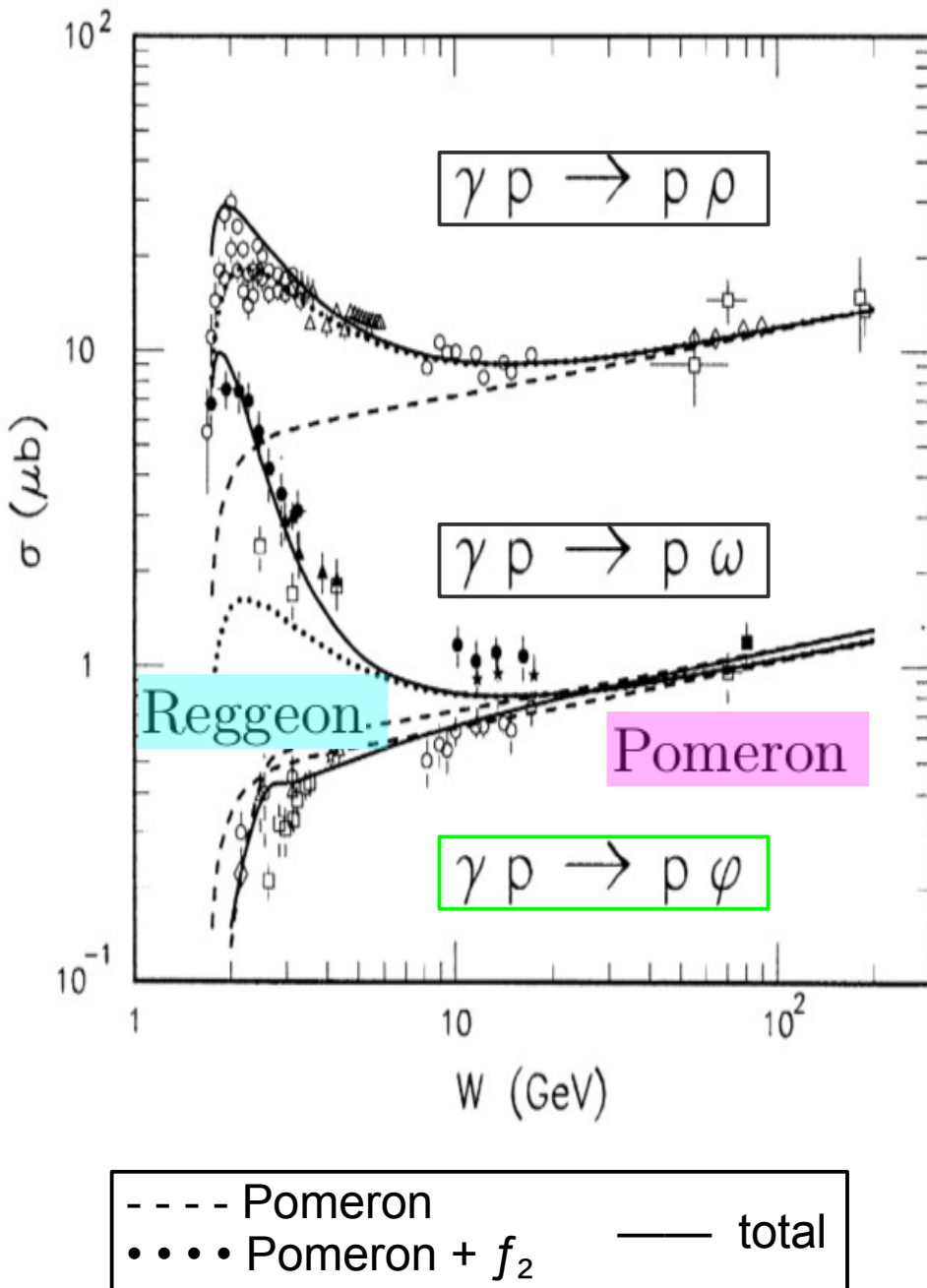
$$\alpha_P(t) \simeq 1.08 + 0.25t$$

$$\sigma \propto s^{\alpha(0)-1} = s^{0.08}$$



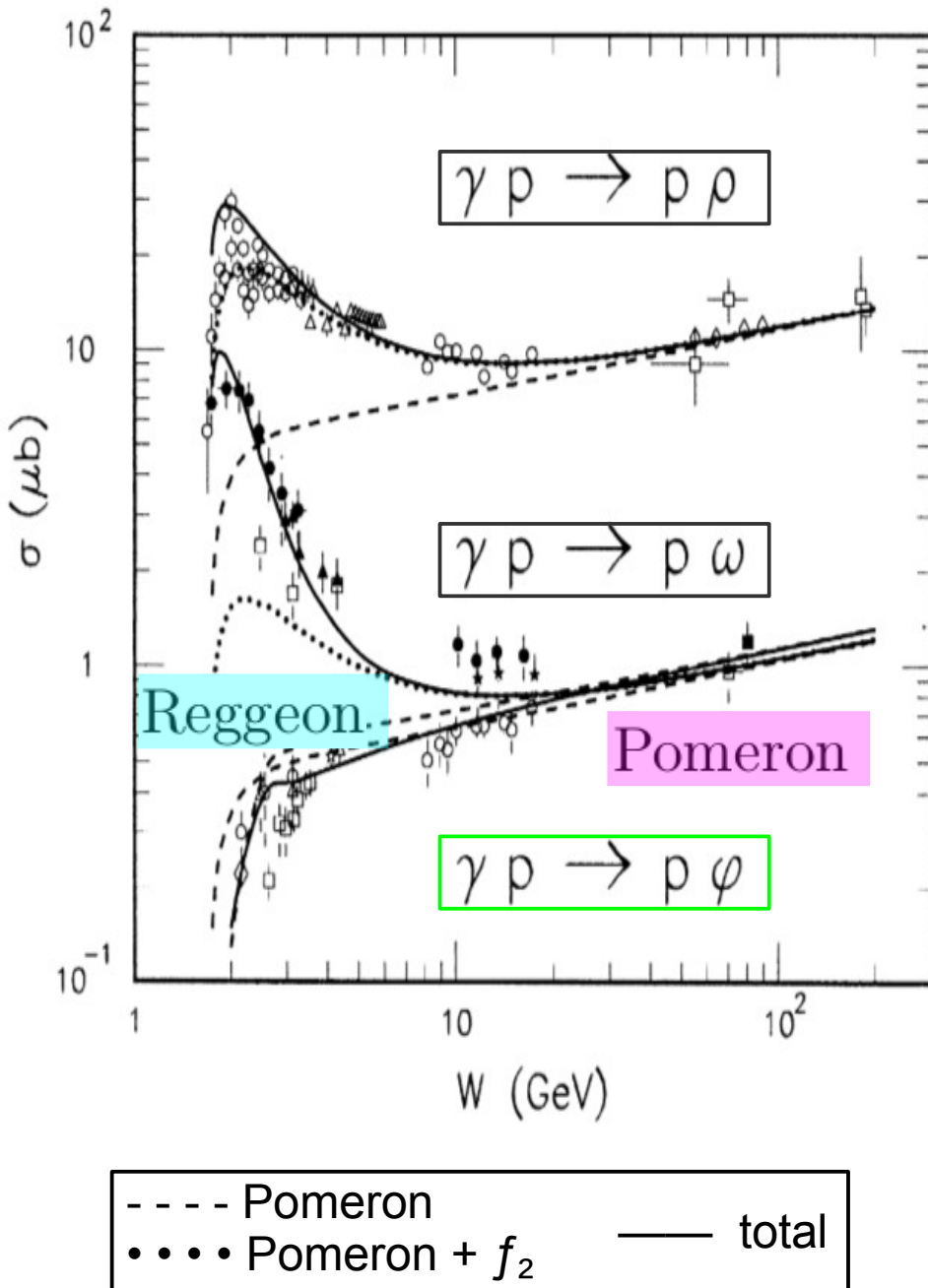


- A maximal Odderon model is proposed to describe the dip and shoulder region for  $pp$  and  $\bar{p}p$  scatterings, respectively.
- This behavior is determined by delicate interference effects.

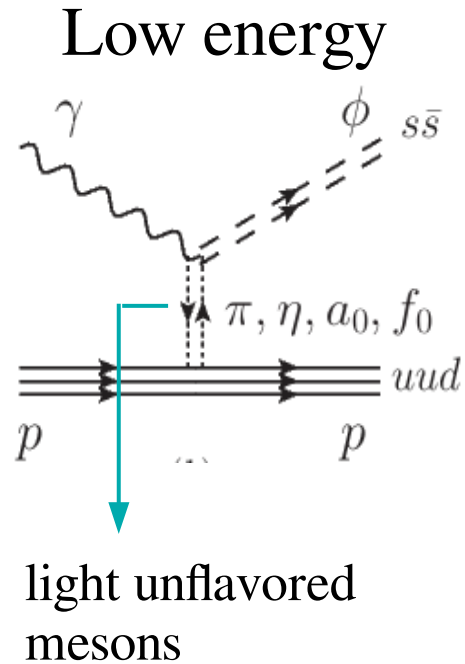


Laget, PLB.489.313(2000)

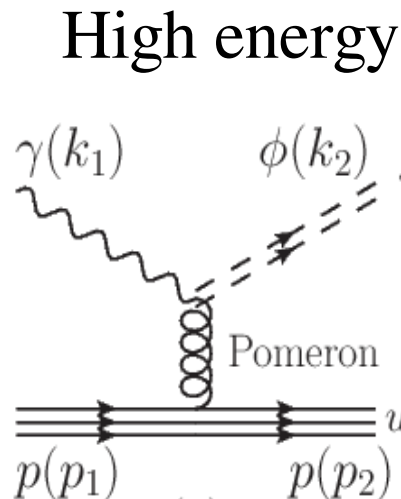




Laget, PLB.489.313(2000)

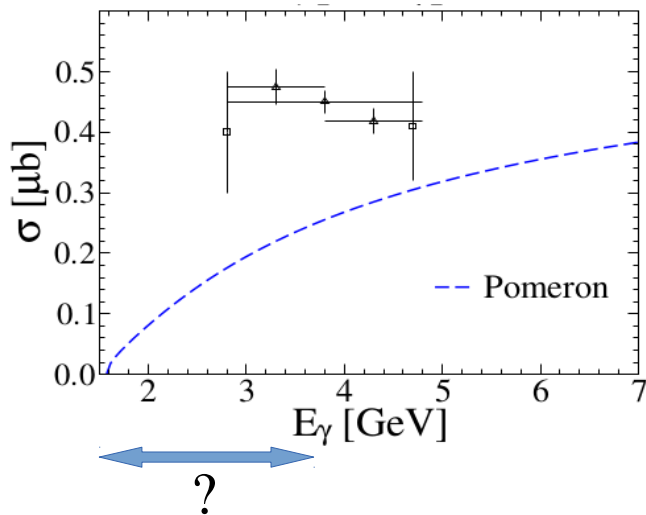


- The dynamics of **Reggeon** is related to non-perturbative QCD in q-q̄ sector.
- OZI suppressed.
- PS(0<sup>-</sup>)  $\pi$  &  $\eta$  exchange
- S(0<sup>+</sup>)  $a_0$  &  $f_0$  exchange

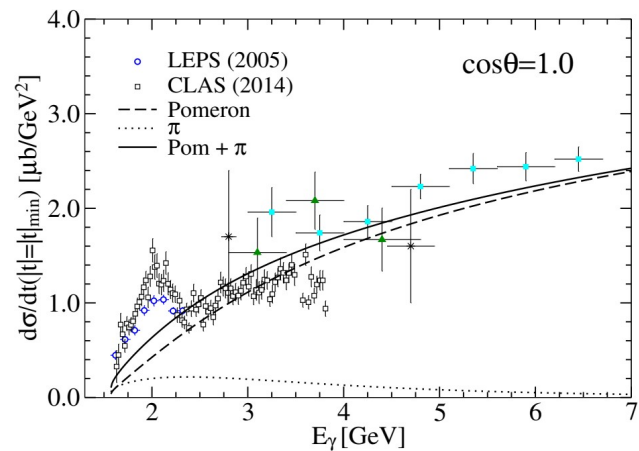


- **Pomeron** is the result of non-perturbative QCD interaction in gluon sector.
- Natural parity (+1).

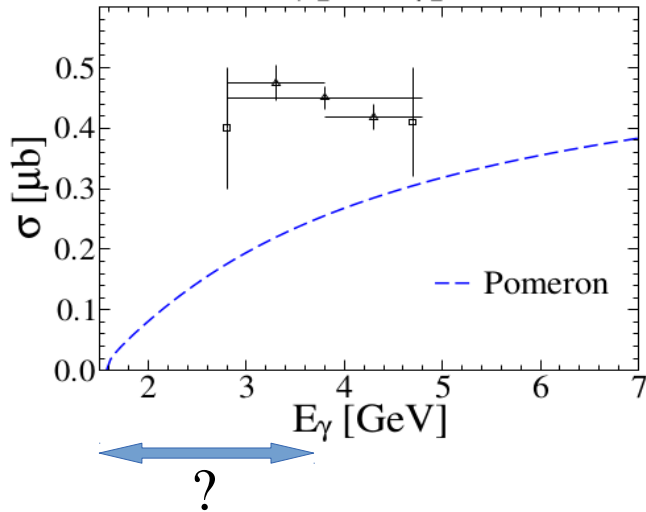
- Pomeron alone is not sufficient to describe low energy regions.



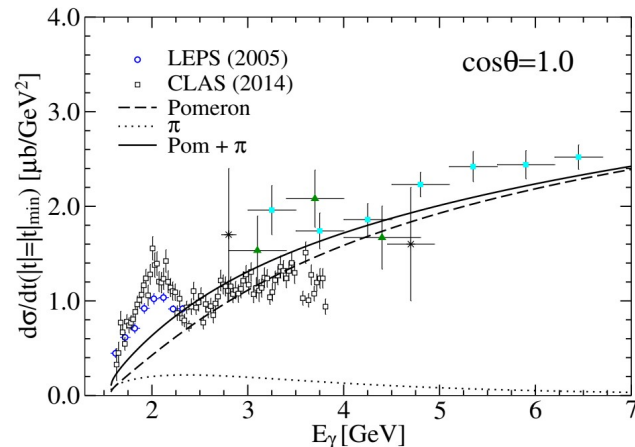
- Only forward angle data existed before.



- Pomeron alone is not sufficient to describe low energy regions.

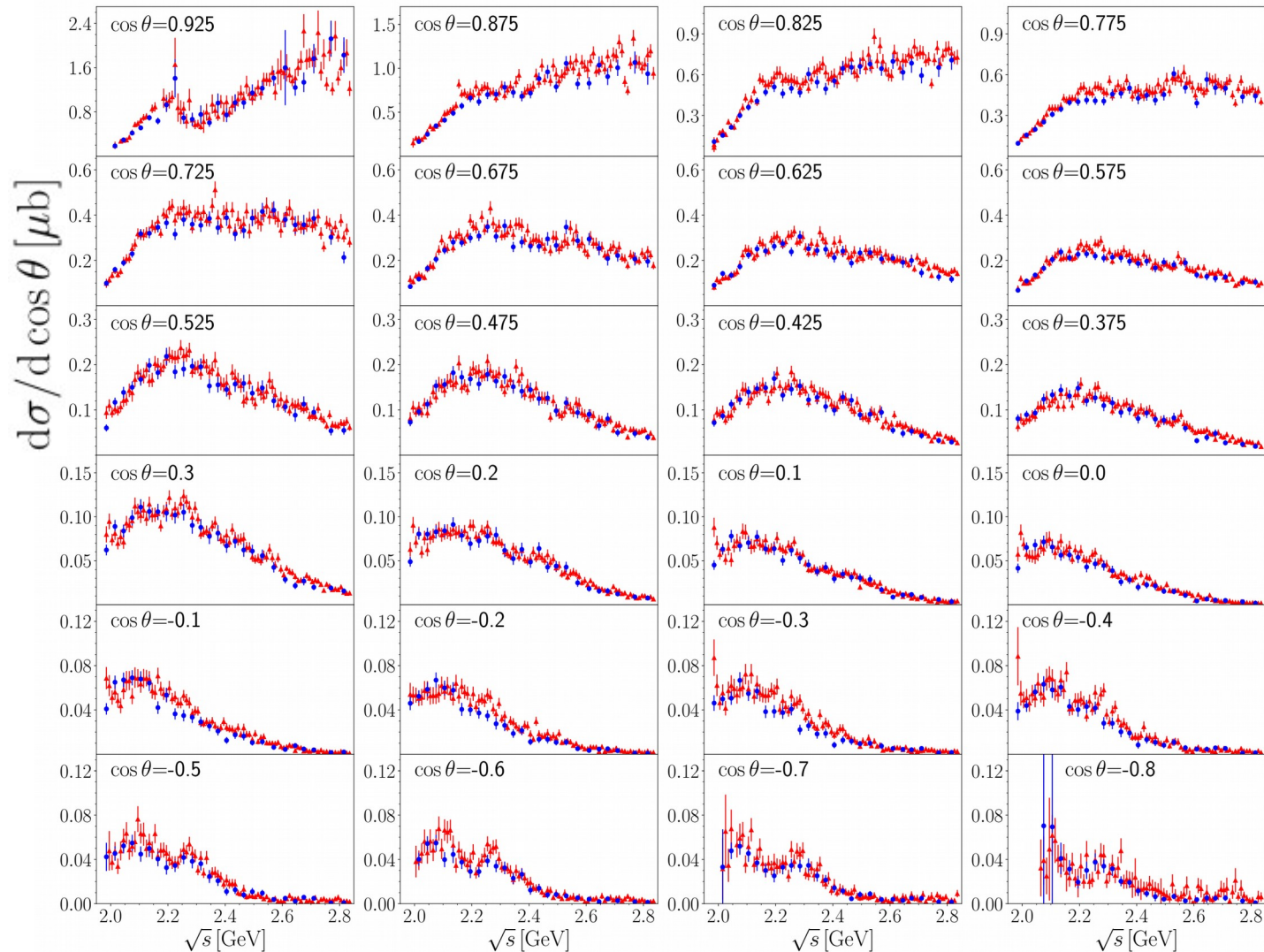


- Only forward angle data existed before.

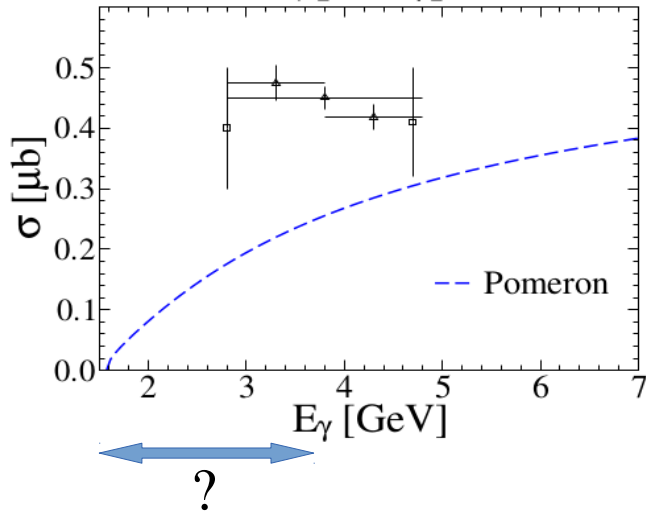


- Abundant data are reported at CLAS at full scattering angles & low energies ( $\sqrt{s} = 1.9\text{-}2.8$  GeV).

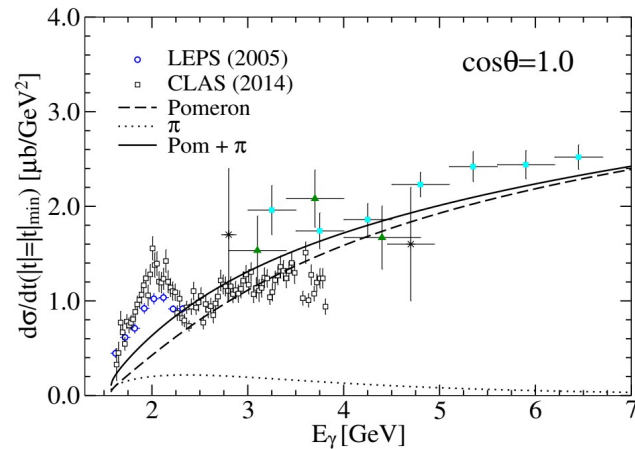
[Seraydaryan, PRC.89.055206] & [Dey, PRC.89.055208] (2014)



- Pomeron alone is not sufficient to describe low energy regions.

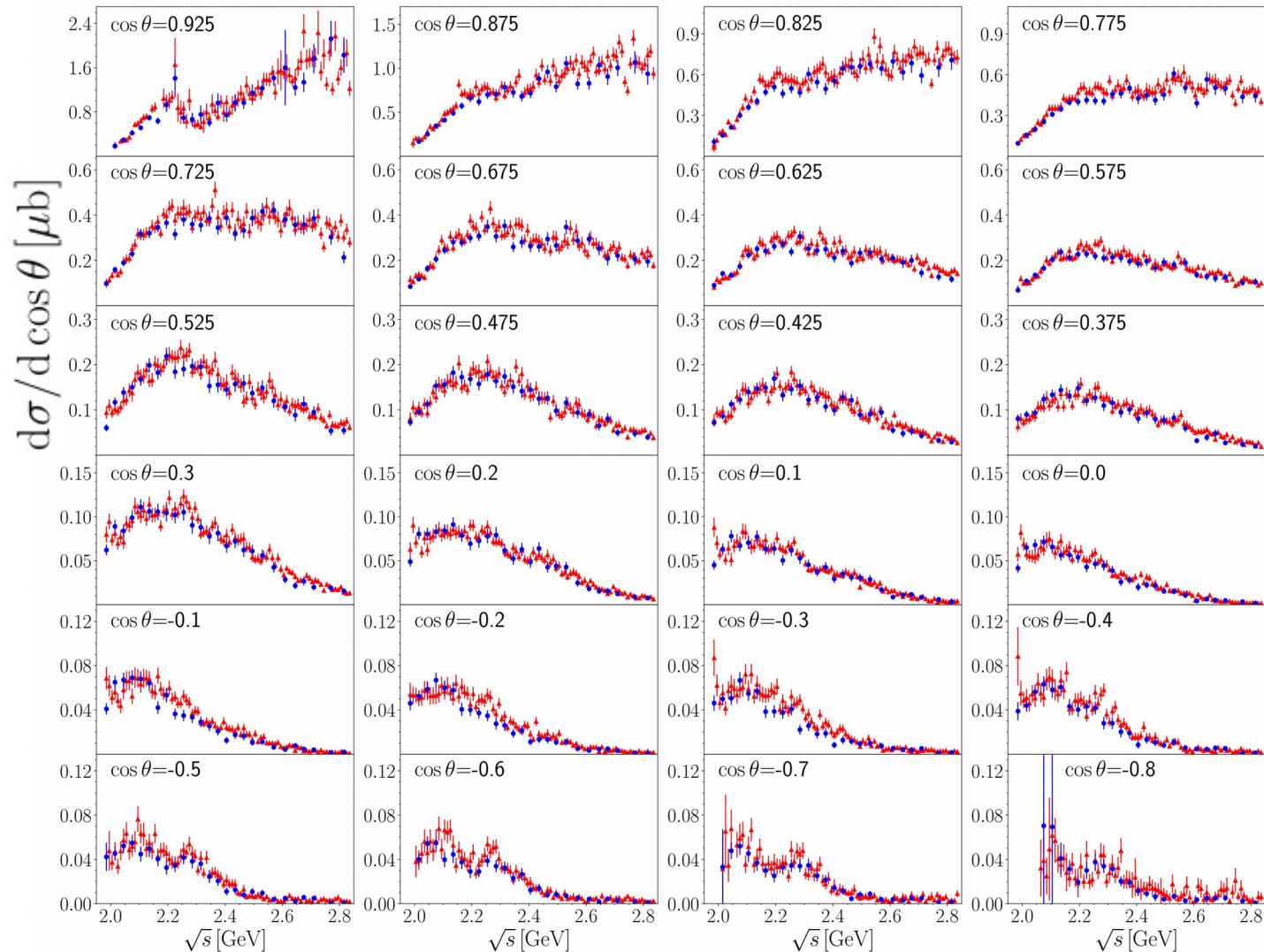


- Only forward angle data existed before.



- Abundant data are reported at CLAS at full scattering angles & low energies ( $\sqrt{s} = 1.9-2.8$  GeV).

[Seraydaryan, PRC.89.055206] & [Dey, PRC.89.055208] (2014)

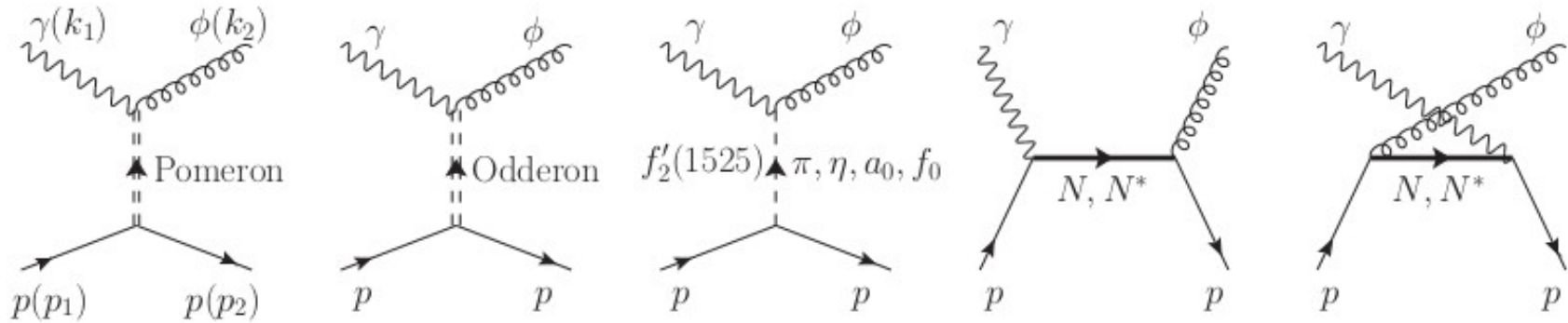


• We need a systematic analysis on  $\phi$  photoproduction.

# Formalism



- Feynman diagrams for  $\gamma p \rightarrow \phi(1020)p$



Previous work: Pomeron + PS( $\pi, \eta$ ) + N + assumed  $N^*$

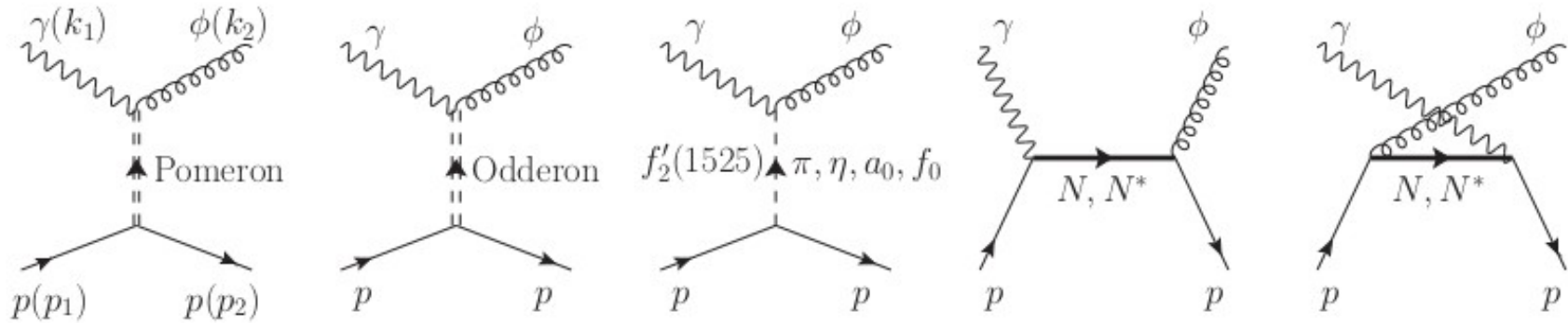
Our work: Pomeron + PS( $\pi, \eta$ ) + N + Odderon + S( $a_0, f_0$ ) +  $f_2'$  + PDG  $N^*$

Pomeron: two-gluon exchange ( $C=P=1$ )

Odderon: three-gluon exchange ( $C=P=-1$ )

- A number of high-energy reactions have been proposed for detecting the Odderon, e.g. “ $\gamma^{(*)} + p \rightarrow \eta_c + p$ ” & “ $\gamma + \gamma \rightarrow M + M$ ”.

• Feynman diagrams for  $\gamma p \rightarrow \phi(1020)p$



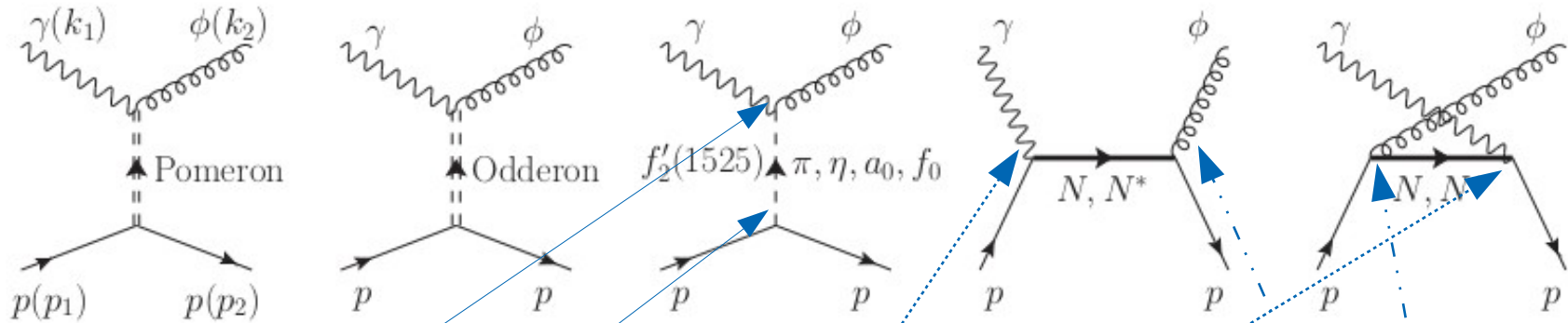
Previous work: Pomeron + PS( $\pi, \eta$ ) + N + assumed  $N^*$

Our work: Pomeron + PS( $\pi, \eta$ ) + N + Odderon + S( $a_0, f_0$ ) +  $f_2'$  + PDG  $N^*$

• Effective Lagrangians

$$\left\{ \begin{array}{l} \mathcal{L}_{\gamma\Phi\phi} = \frac{eg_{\gamma\Phi\phi}}{M_\phi} \epsilon^{\mu\nu\alpha\beta} \partial_\mu A_\nu \partial_\alpha \phi_\beta \Phi, \\ \mathcal{L}_{\gamma S\phi} = \frac{eg_{\gamma S\phi}}{M_\phi} A^{\mu\nu} \phi_{\mu\nu} S, \\ \mathcal{L}_{\Phi NN} = -ig_{\Phi NN} \bar{N} \gamma_5 N \Phi, \\ \mathcal{L}_{SNN} = -g_{SNN} \bar{N} N S, \end{array} \right. \quad \begin{array}{l} \mathcal{L}_{\gamma NN} = -e\bar{N} \left[ \gamma_\mu - \frac{\kappa_N}{2M_N} \sigma_{\mu\nu} \partial^\nu \right] N A^\mu, \\ \mathcal{L}_{\phi NN} = -g_{\phi NN} \bar{N} \left[ \gamma_\mu - \frac{\kappa_{\phi NN}}{2M_N} \sigma_{\mu\nu} \partial^\nu \right] N \phi^\mu \end{array}$$

- Feynman diagrams for  $\gamma p \rightarrow \phi(1020)p$



Previous work: Pomeron + PS( $\pi, \eta$ ) + N + assumed  $N^*$   
 Our work: Pomeron + PS( $\pi, \eta$ ) + N + Odderon + S( $a_0, f_0$ ) +  $f_2'$  + PDG  $N^*$

- Effective Lagrangians

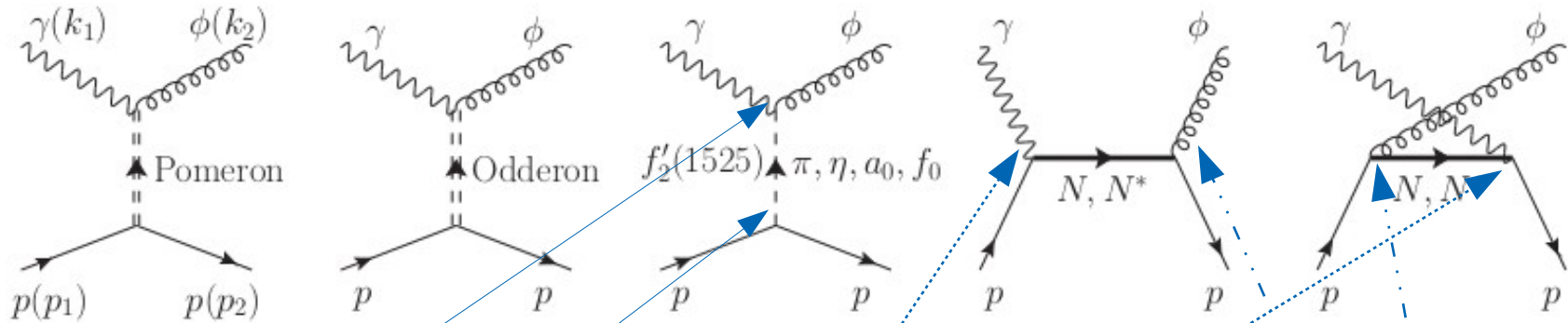
$$\left\{ \begin{aligned} \mathcal{L}_{\gamma\Phi\phi} &= \frac{eg_{\gamma\Phi\phi}}{M_\phi} \epsilon^{\mu\nu\alpha\beta} \partial_\mu A_\nu \partial_\alpha \phi_\beta \Phi, \\ \mathcal{L}_{\gamma S\phi} &= \frac{eg_{\gamma S\phi}}{M_\phi} A^{\mu\nu} \phi_{\mu\nu} S, \\ \mathcal{L}_{\Phi NN} &= -ig_{\Phi NN} \bar{N} \gamma_5 N \Phi, \\ \mathcal{L}_{SNN} &= -g_{SNN} \bar{N} N S, \end{aligned} \right.$$

$$\mathcal{L}_{\gamma NN} = -e\bar{N} \left[ \gamma_\mu - \frac{\kappa_N}{2M_N} \sigma_{\mu\nu} \partial^\nu \right] N A^\mu,$$

$$\mathcal{L}_{\phi NN} = -g_{\phi NN} \bar{N} \left[ \gamma_\mu - \frac{\kappa_{\phi NN}}{2M_N} \sigma_{\mu\nu} \partial^\nu \right] N \phi^\mu$$



- Feynman diagrams for  $\gamma p \rightarrow \phi(1020)p$



Previous work: Pomeron + PS( $\pi, \eta$ ) + N + assumed  $N^*$   
 Our work: Pomeron + PS( $\pi, \eta$ ) + N + Odderon + S( $a_0, f_0$ ) +  $f_2'$  + PDG  $N^*$

- Effective Lagrangians

$$\begin{cases}
 \mathcal{L}_{\gamma\Phi\phi} = \frac{eg_{\gamma\Phi\phi}}{M_\phi} \epsilon^{\mu\nu\alpha\beta} \partial_\mu A_\nu \partial_\alpha \phi_\beta \Phi, & \mathcal{L}_{\gamma NN} = -e\bar{N} \left[ \gamma_\mu - \frac{\kappa_N}{2M_N} \sigma_{\mu\nu} \partial^\nu \right] N A^\mu, \\
 \mathcal{L}_{\gamma S\phi} = \frac{eg_{\gamma S\phi}}{M_\phi} A^{\mu\nu} \phi_{\mu\nu} S, & \\
 \mathcal{L}_{\Phi NN} = -ig_{\Phi NN} \bar{N} \gamma_5 N \Phi, & \mathcal{L}_{\phi NN} = -g_{\phi NN} \bar{N} \left[ \gamma_\mu - \frac{\kappa_{\phi NN}}{2M_N} \sigma_{\mu\nu} \partial^\nu \right] N \phi^\mu, \\
 \mathcal{L}_{SNN} = -g_{SNN} \bar{N} N S, &
 \end{cases}$$

- Form factors are considered to dress the interaction vertices.

meson exchange

$$F_{\Phi,S}(t) = \frac{\Lambda_{\Phi,S}^2 - M_{\Phi,S}^2}{\Lambda_{\Phi,S}^2 - t}$$

N exchange

$$F_N(x) = \frac{\Lambda_N^4}{\Lambda_N^4 + (x - M_N^2)^2}$$

$N^*$  exchange (Gaussian form)

$$F_{N^*}(x) = \exp \left[ -\frac{(x - M_{N^*}^2)^2}{\Lambda_{N^*}^4} \right]$$

- scattering amplitude:

$$\mathcal{M} = \varepsilon_\nu^* \bar{u}_{N'} \mathcal{M}^{\mu\nu} u_N \epsilon_\mu \quad \mathcal{M}^{\mu\nu} = -M(s, t) \Gamma^{\mu\nu}$$

- transition operator:

$$\Gamma^{\mu\nu} = \not{k}_1 \left( g^{\mu\nu} - \frac{k_2^\mu k_2^\nu}{k_2^2} \right) - \gamma^\mu \left( k_1^\nu - \frac{k_1 \cdot k_2 k_2^\nu}{k_2^2} \right) - \left[ k_2^\mu - \frac{k_1 \cdot k_2 (p_1^\mu + p_2^\mu)}{k_1 \cdot (p_1 + p_2)} \right] \left( \gamma^\nu - \frac{\not{k}_2 k_2^\nu}{k_2^2} \right)$$

- scalar function:  $M(s, t) = C_P F_1(t) F_2(t) \frac{1}{s} \left( \frac{s - s_{th}}{s_P} \right)^{\alpha_P(t)} \exp \left[ -\frac{i\pi}{2} \alpha_P(t) \right]$

- form factors:  $F_1(t) = \frac{4M_N^2 - a_N^2 t}{(4M_N^2 - t)(1 - t/t_0)^2}$ ,  $F_2(t) = \frac{2\mu_0^2}{(1 - t/M_\phi^2)(2\mu_0^2 + M_\phi^2 - t)}$

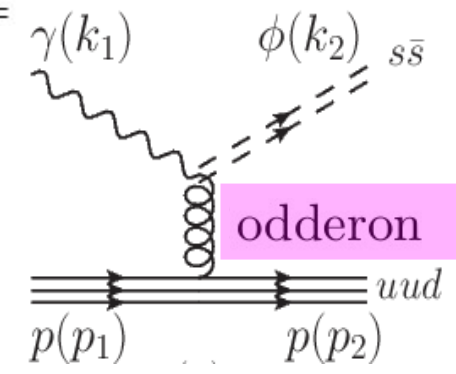
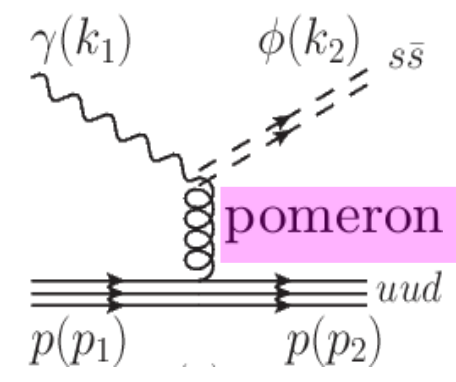
	$\alpha_P(t)$	$s_P$ [GeV <sup>2</sup> ]	$s_{th}$ [GeV <sup>2</sup> ]	$C_P$	$a_N^2$	$\mu_0^2$	$t_0$ [GeV <sup>2</sup> ]
Titov(2003)	1.08+0.25t	4	0	3.65	2.8	1.1	0.7
Titov(2007)	"	"	"	3.20	4	"	"
Kiswandhi(2012)	"	$(M_N + M_\phi)^2$	1.3	3.65	2.8	"	"
In this work	"	"	0	3.0	6.0	"	"

- scattering amplitude:

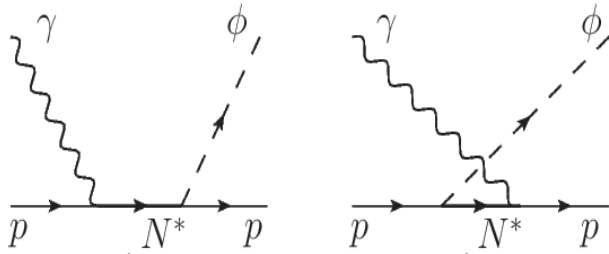
$$\mathcal{M} = \varepsilon_\nu^* \bar{u}_{N'} \mathcal{M}^{\mu\nu} u_N \epsilon_\mu \quad \mathcal{M}^{\mu\nu} = -iM(s, t) \Gamma^{\mu\nu}$$

- Pomeron & Odderon trajectories:

$$\alpha_P(t) = 1.08 + (0.25 \text{ GeV}^{-2})t, \quad \alpha_O(t) = 0.95 + (0.25 \text{ GeV}^{-2})t$$



- We choose N(2100), N(2120) & N(2300) from “PDG 2018” to describe two bump structures at backward angles.



- Effective Lagrangians

$$\mathcal{L}_{\gamma NN^*} = \frac{eg_{\gamma NN^*}}{2M_N} \bar{N}^* (\sigma \cdot F) N + \text{h.c.}$$

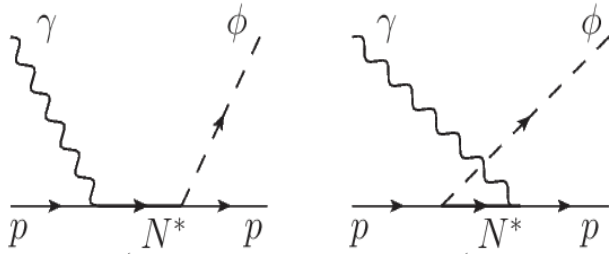
$$\mathcal{L}_{\phi NR} = g_{\phi NN^*} \bar{N} \phi N^* + \text{h.c.}$$

- $\Gamma_{N^*} = (200-300) \text{ MeV}$

## PDG 2018

	N(2000)	5/2 <sup>+</sup>	**
	N(2040)	3/2 <sup>+</sup>	*
	N(2060)	5/2 <sup>-</sup>	***
→	N(2100)	1/2 <sup>+</sup>	***
→	N(2120)	3/2 <sup>-</sup>	***
	N(2190)	7/2 <sup>-</sup>	****
	N(2220)	9/2 <sup>+</sup>	****
	N(2250)	9/2 <sup>-</sup>	****
→	N(2300)	1/2 <sup>+</sup>	**
	N(2570)	5/2 <sup>-</sup>	**
	N(2600)	11/2 <sup>-</sup>	***
	N(2700)	13/2 <sup>+</sup>	**

- We choose N(2100), N(2120) & N(2300) from “PDG 2018” to describe two bump structures at backward angles.



- Effective Lagrangians

$$\mathcal{L}_{\gamma NN^*} = \frac{eg_{\gamma NN^*}}{2M_N} \bar{N}^* (\sigma \cdot F) N + \text{h.c.}$$

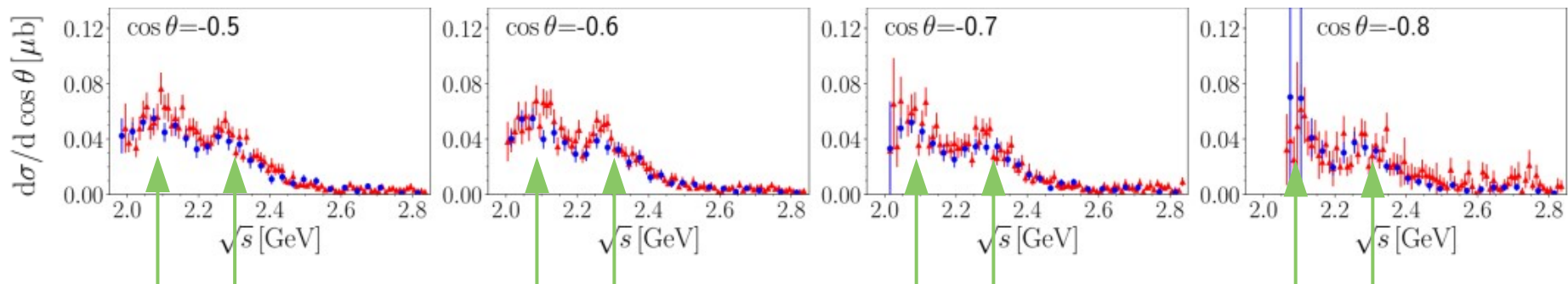
$$\mathcal{L}_{\phi NR} = g_{\phi NN^*} \bar{N} \phi N^* + \text{h.c.}$$

- $\Gamma_{N^*} = (200-300) \text{ MeV}$

## PDG 2018

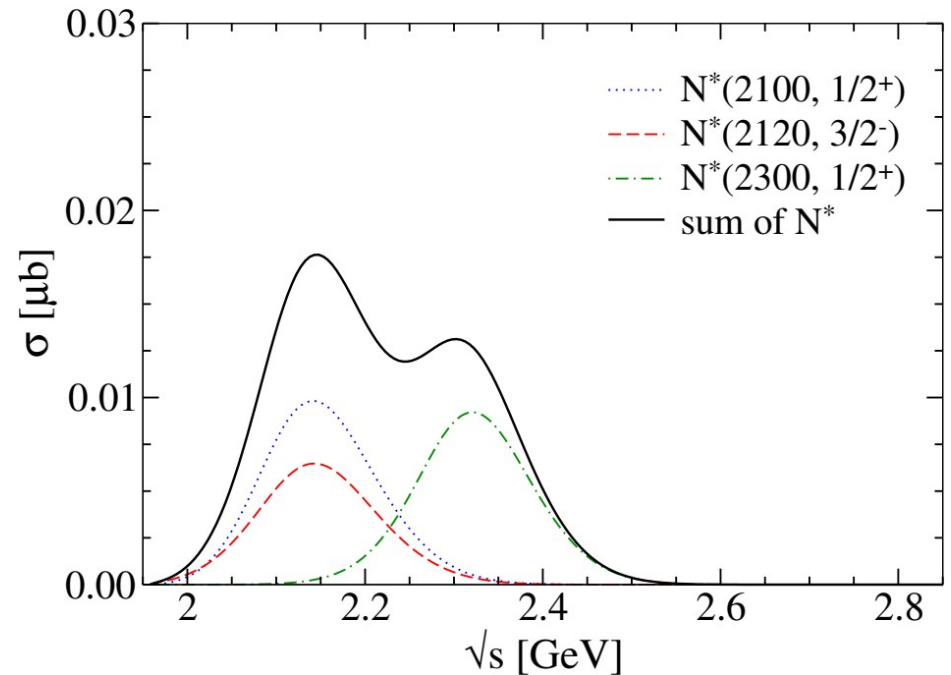
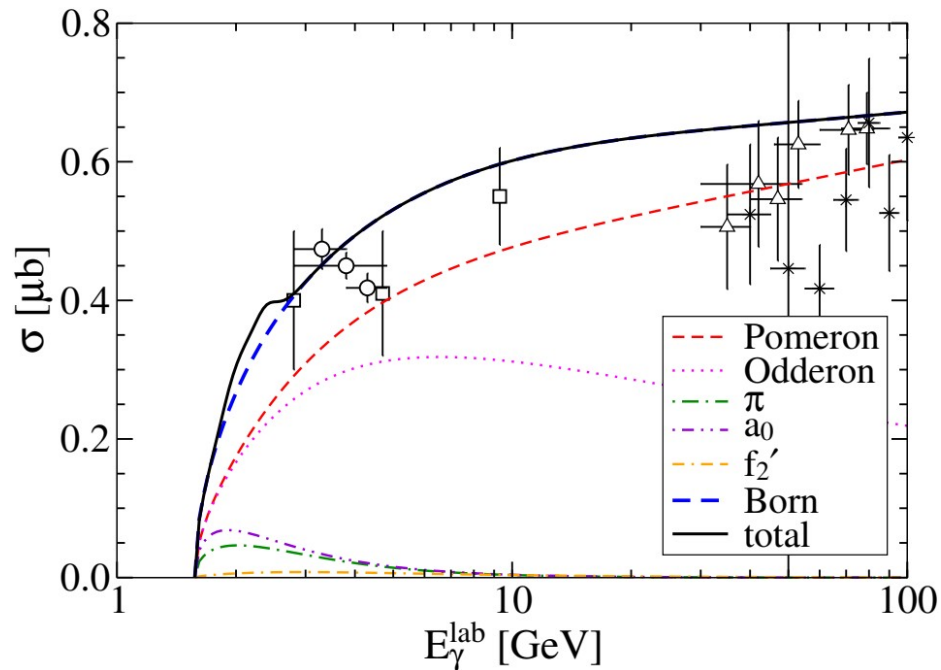
	N(2000)	5/2 <sup>+</sup>	**
	N(2040)	3/2 <sup>+</sup>	*
	N(2060)	5/2 <sup>-</sup>	***
→	N(2100)	1/2 <sup>+</sup>	***
→	N(2120)	3/2 <sup>-</sup>	***
	N(2190)	7/2 <sup>-</sup>	****
	N(2220)	9/2 <sup>+</sup>	****
	N(2250)	9/2 <sup>-</sup>	****
→	N(2300)	1/2 <sup>+</sup>	**
	N(2570)	5/2 <sup>-</sup>	**
	N(2600)	11/2 <sup>-</sup>	***
	N(2700)	13/2 <sup>+</sup>	**

- Two bump structures are located near their pole positions, i.e.  $\sqrt{s} \approx 2.1$  &  $2.3 \text{ GeV}$ .
- We expect only lower partial waves would be important.



# Numerical Results

## Total cross section



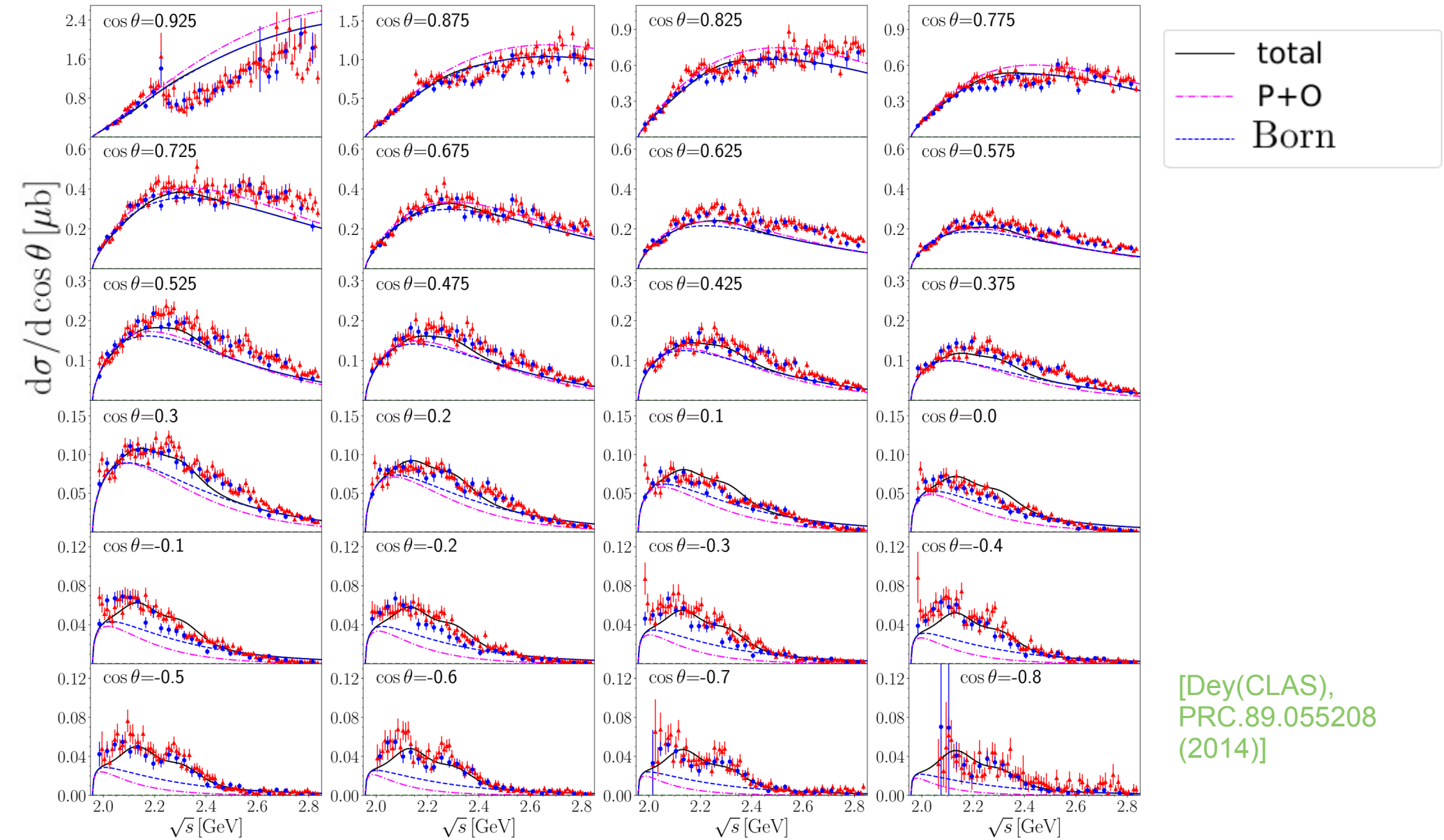
$$\mathcal{M}_{\text{total}} = \sum_i \mathcal{M}_i^{\text{Born}} + \sum_j \mathcal{C}_j \mathcal{M}_j^{N^*}$$

$$i = (\mathbb{P}, \mathbb{O}, \pi, \eta, a_0, f_0, f_2')$$

$$j = (N^*(2100, 1/2^+), \\ N^*(2120, 3/2^-), \\ N^*(2300, 1/2^+))$$

- The total cross section is almost governed by Pomeron and Odderon exchanges.
- Other contributions are small to the total cross section but come into play significantly for the “differential cross sections” and “spin-density matrices”.

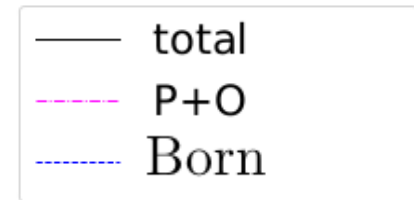
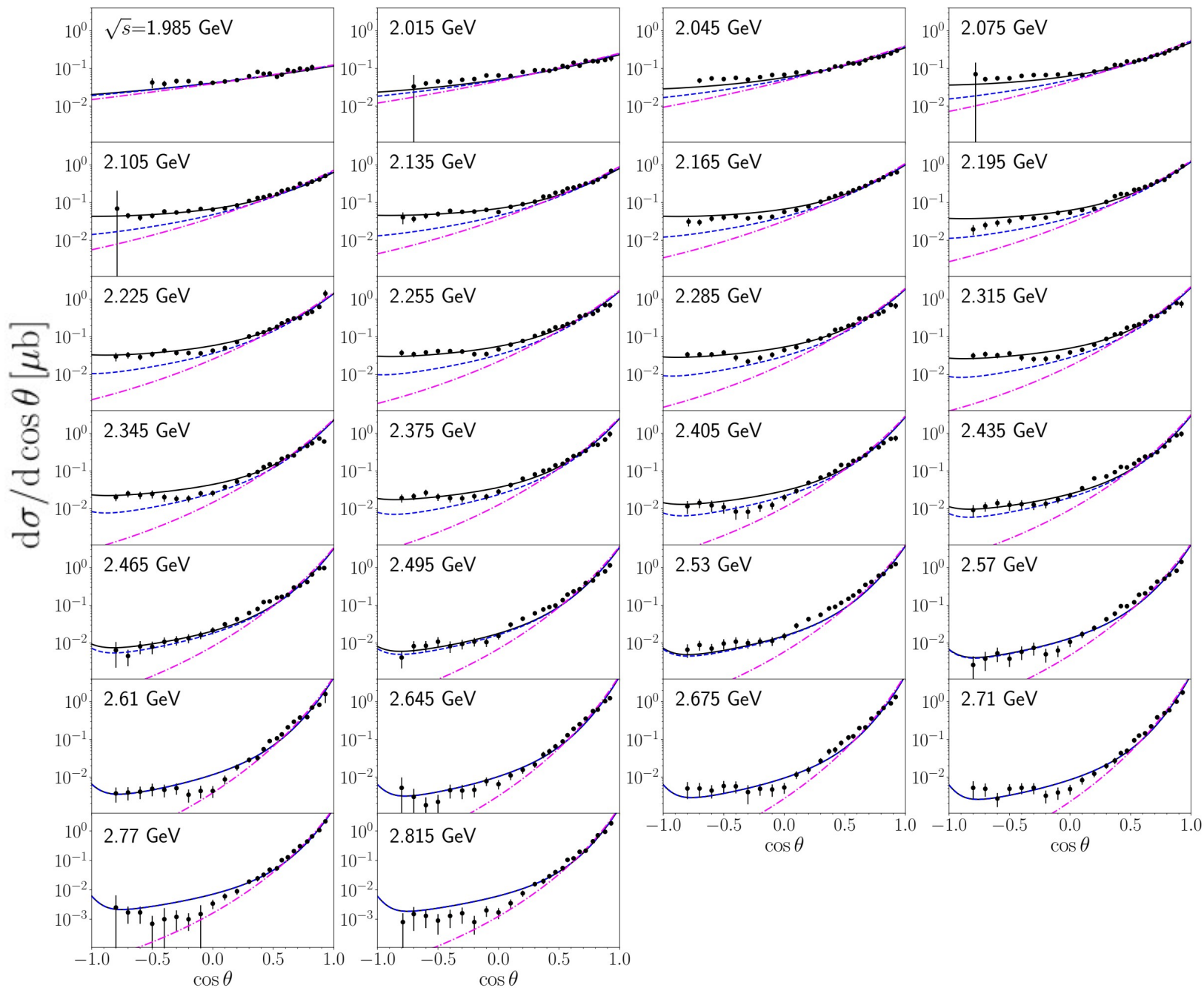
# Differential cross sections (1)



- PS- and S-meson exchanges, respectively, make constructive and destructive interference effects with the dominant Pomeron and Odderon contributions.
- Three  $N^*$  contributions improve the results at backward angles remarkably.



# Differential cross sections (2)



[Dey(CLAS),  
PRC.89.055208  
(2014)]



- SDMEs in terms of the helicity amplitudes

$$\rho_{\lambda\lambda'}^0 = \frac{1}{N} \sum_{\lambda_\gamma, \lambda_i, \lambda_f} \mathcal{M}_{\lambda_f \lambda; \lambda_i \lambda_\gamma} \mathcal{M}_{\lambda_f \lambda'; \lambda_i \lambda_\gamma}^*$$

$$\rho_{\lambda\lambda'}^1 = \frac{1}{N} \sum_{\lambda_\gamma, \lambda_i, \lambda_f} \mathcal{M}_{\lambda_f \lambda; \lambda_i - \lambda_\gamma} \mathcal{M}_{\lambda_f \lambda'; \lambda_i \lambda_\gamma}^*$$

$$\rho_{\lambda\lambda'}^2 = \frac{i}{N} \sum_{\lambda_\gamma, \lambda_i, \lambda_f} \lambda_\gamma \mathcal{M}_{\lambda_f \lambda; \lambda_i - \lambda_\gamma} \mathcal{M}_{\lambda_f \lambda'; \lambda_i \lambda_\gamma}^*$$

$$\rho_{\lambda\lambda'}^3 = \frac{1}{N} \sum_{\lambda_\gamma, \lambda_i, \lambda_f} \lambda_\gamma \mathcal{M}_{\lambda_f \lambda; \lambda_i \lambda_\gamma} \mathcal{M}_{\lambda_f \lambda'; \lambda_i \lambda_\gamma}^*$$

- normalization factor

$$N = \sum |\mathcal{M}_{\lambda_f \lambda; \lambda_i \lambda_\gamma}|^2$$

- symmetry relation

$$\rho_{\lambda\lambda'}^\alpha = (-1)^{\lambda - \lambda'} \rho_{-\lambda - \lambda'}^\alpha \quad \text{for } (\alpha = 0, 1),$$

$$\rho_{\lambda\lambda'}^\alpha = -(-1)^{\lambda - \lambda'} \rho_{-\lambda - \lambda'}^\alpha \quad \text{for } (\alpha = 2, 3)$$

- SDMEs in terms of the helicity amplitudes

$$\rho_{\lambda\lambda'}^0 = \frac{1}{N} \sum_{\lambda_\gamma, \lambda_i, \lambda_f} \mathcal{M}_{\lambda_f \lambda; \lambda_i \lambda_\gamma} \mathcal{M}_{\lambda_f \lambda'; \lambda_i \lambda_\gamma}^*$$

$$\rho_{\lambda\lambda'}^1 = \frac{1}{N} \sum_{\lambda_\gamma, \lambda_i, \lambda_f} \mathcal{M}_{\lambda_f \lambda; \lambda_i - \lambda_\gamma} \mathcal{M}_{\lambda_f \lambda'; \lambda_i \lambda_\gamma}^*$$

$$\rho_{\lambda\lambda'}^2 = \frac{i}{N} \sum_{\lambda_\gamma, \lambda_i, \lambda_f} \lambda_\gamma \mathcal{M}_{\lambda_f \lambda; \lambda_i - \lambda_\gamma} \mathcal{M}_{\lambda_f \lambda'; \lambda_i \lambda_\gamma}^*$$

$$\rho_{\lambda\lambda'}^3 = \frac{1}{N} \sum_{\lambda_\gamma, \lambda_i, \lambda_f} \lambda_\gamma \mathcal{M}_{\lambda_f \lambda; \lambda_i \lambda_\gamma} \mathcal{M}_{\lambda_f \lambda'; \lambda_i \lambda_\gamma}^*$$

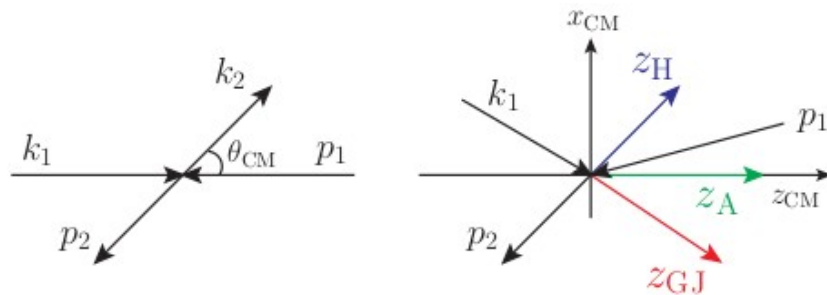
- normalization factor

$$N = \sum |\mathcal{M}_{\lambda_f \lambda; \lambda_i \lambda_\gamma}|^2$$

- symmetry relation

$$\rho_{\lambda\lambda'}^\alpha = (-1)^{\lambda-\lambda'} \rho_{-\lambda-\lambda'}^\alpha \quad \text{for } (\alpha = 0, 1),$$

$$\rho_{\lambda\lambda'}^\alpha = -(-1)^{\lambda-\lambda'} \rho_{-\lambda-\lambda'}^\alpha \quad \text{for } (\alpha = 2, 3)$$



**Adair frame:** z axis is parallel to the incoming photon momentum in the CM frame.

**Helicity frame:** z axis is antiparallel to the momentum of the outgoing nucleon.

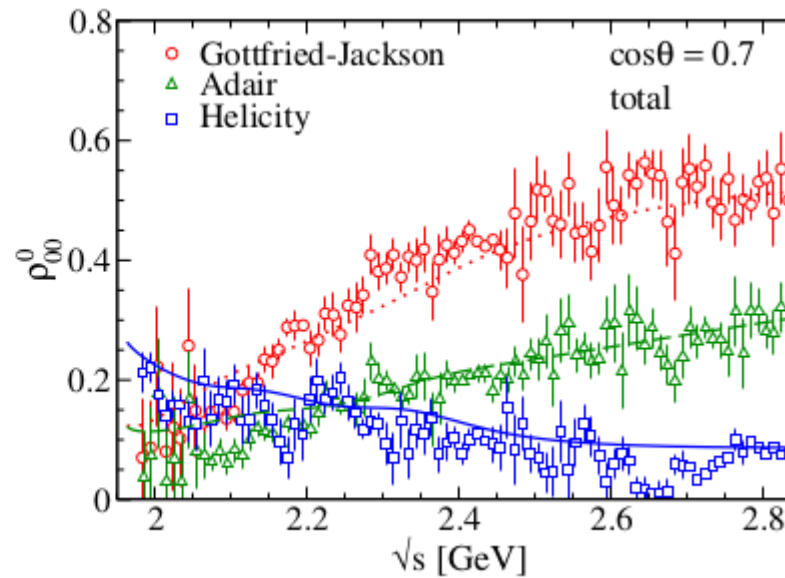
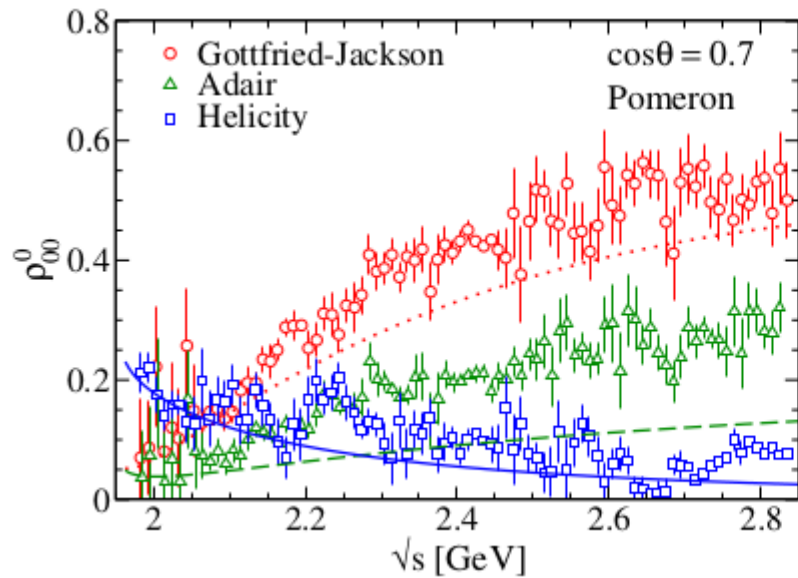
It is in favor of s-channel helicity conservation (SCHC).

**Gottfried-Jackson frame:** z axis is parallel to the momentum of the incoming photon.

It is in favor of t-channel helicity conservation (TCHC).

- center of mass frame
- $\phi$ -meson rest frame

# Spin-density matrix elements (1)

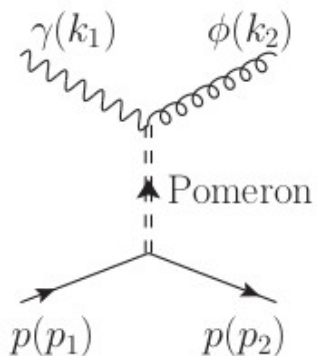


[Dey(CLAS),  
PRC.89.055208  
(2014)]

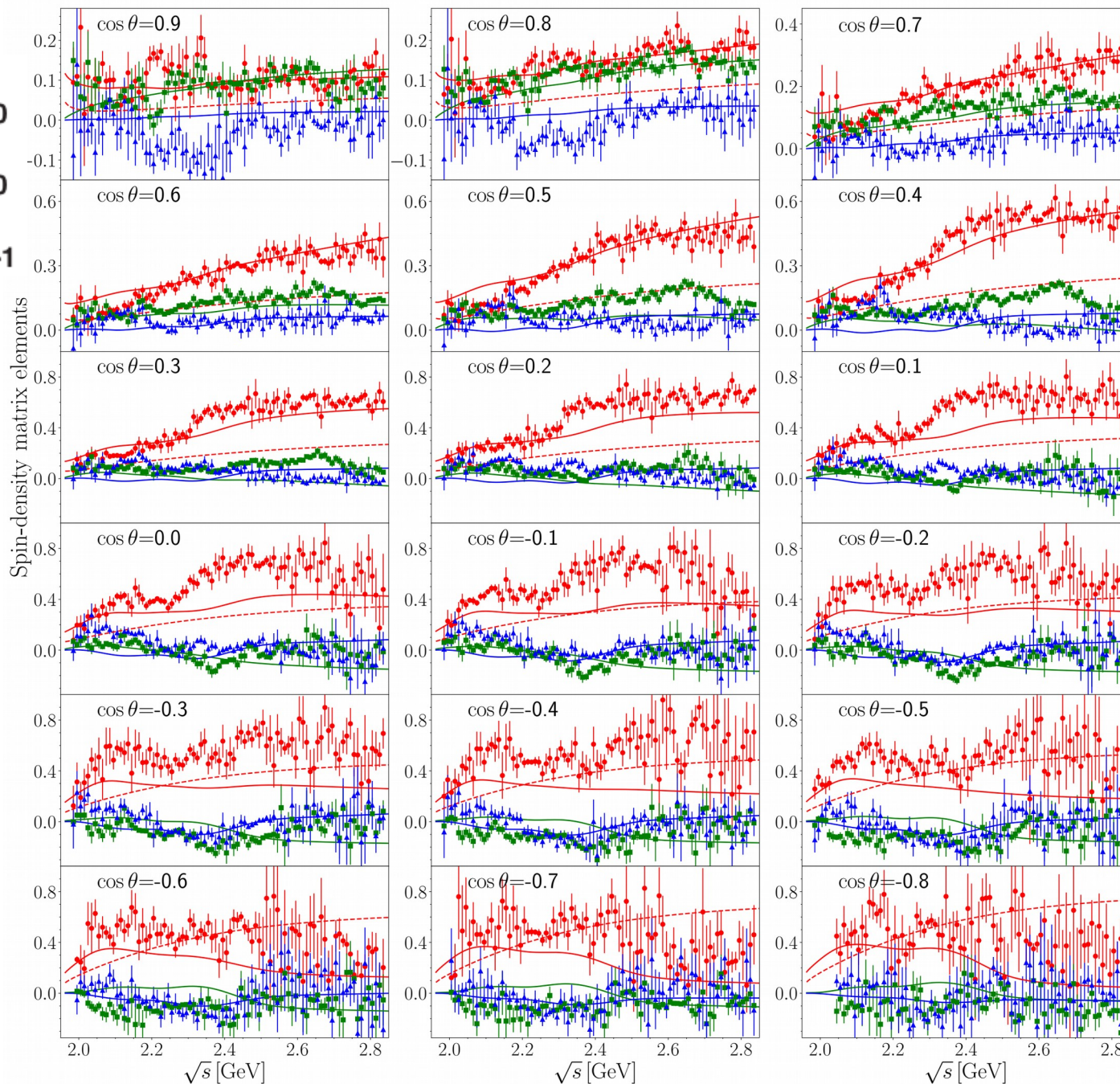
- $\rho_{00}^0$  is nonzero in all three frames and thus exhibits strong deviation from TCHC, implying nonzero helicity flip ( $\rho_{00}^0 \propto |\mathcal{M}_{\lambda_\gamma=1, \lambda_\phi=0}|^2 + |\mathcal{M}_{\lambda_\gamma=-1, \lambda_\phi=0}|^2$ ).

- The inclusion of  $S(a_0, f_0)$ - &  $f_2'$ -mesons is essential to improve the results.

- Pomeron alone is not sufficient.



[Adair frame]



- forward angle:  
Pomeron alone is not enough.  
S(a<sub>0</sub>,f<sub>0</sub>)- & f<sub>2</sub>'-mesons improves the results.
- backward angle:  
N\* exchange describes the bump structure.

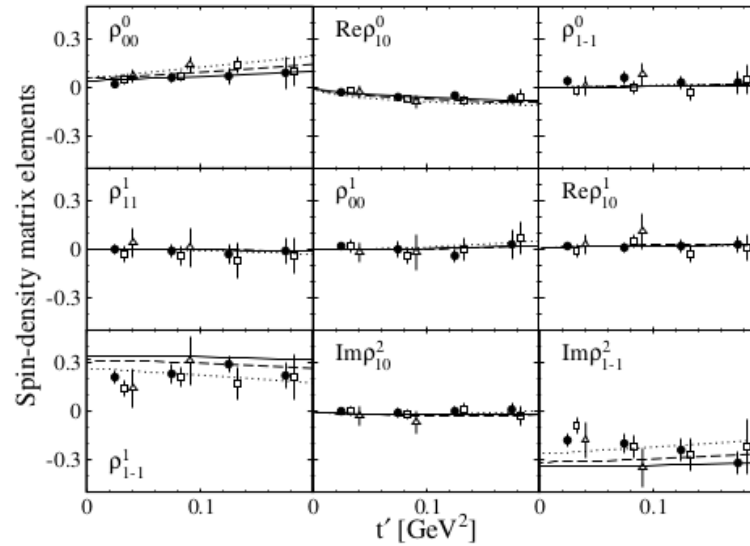
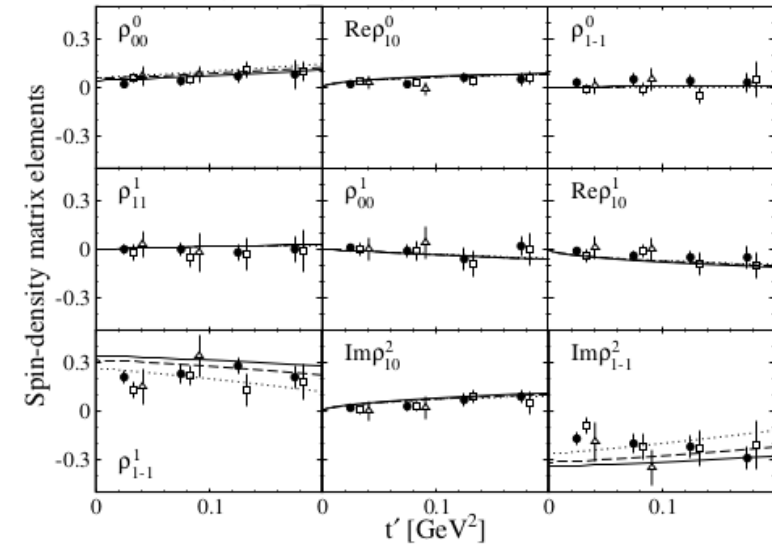
[Dey(CLAS),  
PRC.89.05208  
(2014)]

# Spin-density matrix elements (3)

- △  $1.77 < E_{\gamma}^{lab} < 1.97$     ····  $E_{\gamma}^{lab} = 1.87$  GeV
- $1.97 < E_{\gamma}^{lab} < 2.17$     - - -  $E_{\gamma}^{lab} = 2.07$  GeV
- $2.17 < E_{\gamma}^{lab} < 2.37$     —  $E_{\gamma}^{lab} = 2.27$  GeV

total  
Adair frame

total  
Helicity frame



[Chang(LEPS),  
PRC.82.015205  
(2010)]

$$-\text{Im}[\rho_{1-1}^2] \approx \rho_{1-1}^1$$

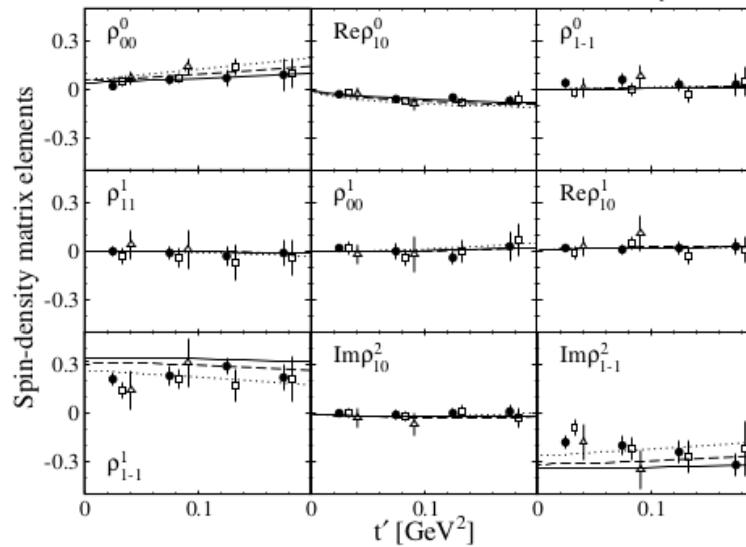
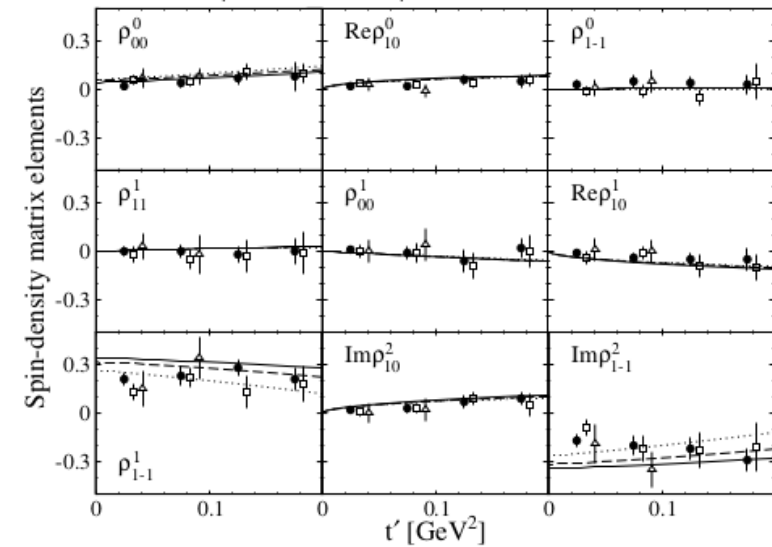


# Spin-density matrix elements (3)

$\triangle$   $1.77 < E_{\gamma}^{\text{lab}} < 1.97$      $\cdots$   $E_{\gamma}^{\text{lab}} = 1.87$  GeV  
 $\square$   $1.97 < E_{\gamma}^{\text{lab}} < 2.17$      $-\cdot-$   $E_{\gamma}^{\text{lab}} = 2.07$  GeV  
 $\bullet$   $2.17 < E_{\gamma}^{\text{lab}} < 2.37$      $-$   $E_{\gamma}^{\text{lab}} = 2.27$  GeV

total  
Adair frame

total  
Helicity frame

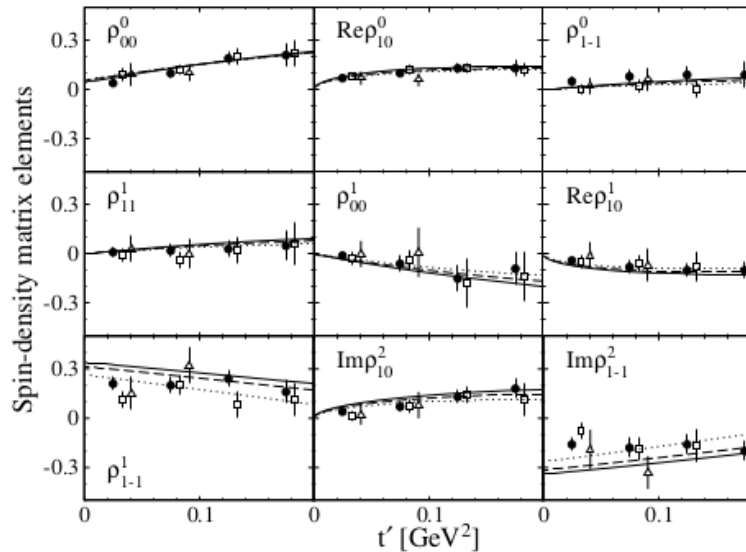
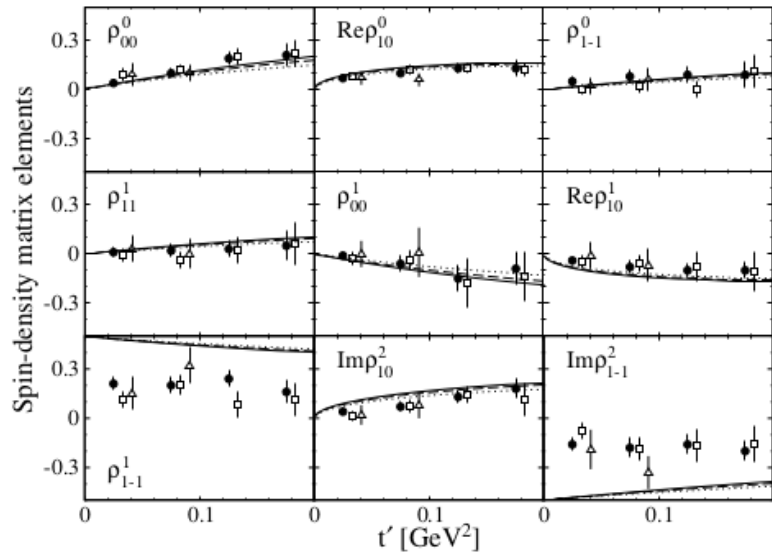


[Chang(LEPS),  
PRC.82.015205  
(2010)]

$$-\text{Im}[\rho_{1-1}^2] \approx \rho_{1-1}^1$$

Pomeron    Gottfried-Jackson frame

total    Gottfried-Jackson frame



- Pomeron exchange
 
$$\rho_{1-1}^1 \simeq \frac{1}{2}(1 - \rho_{00}^0)$$

- Relative strength of N & U parity exchange processes

$$\rho_{1-1}^1 = \frac{1}{2} \frac{\sigma^N - \sigma^U}{\sigma^N + \sigma^U}$$

- GJ frame is useful to test TCHC.

# Summary

- ◇  $\varphi$  photoproduction,  $\gamma p \rightarrow \varphi(1020)p$ , is reanalyzed with effective Lagrangians .
- ◇ Abundant CLAS(2014) data are reported at full angles & low energies.
- ◇ Various contributions from t-channel exchanges and  $N^*$  exchange are considered in addition to the dominant Pomeron exchange.
  - ⇒ Odderon
  - ⇒  $f'_2(1525)$  trajectories
  - ⇒ pseudoscalar meson ( $\pi, \eta$ )
  - ⇒ scalar meson ( $a_0, f_0$ )
- ◇ Extension to other vector-meson ( $\rho, \omega$ ) photo- and electro-production mechanisms.



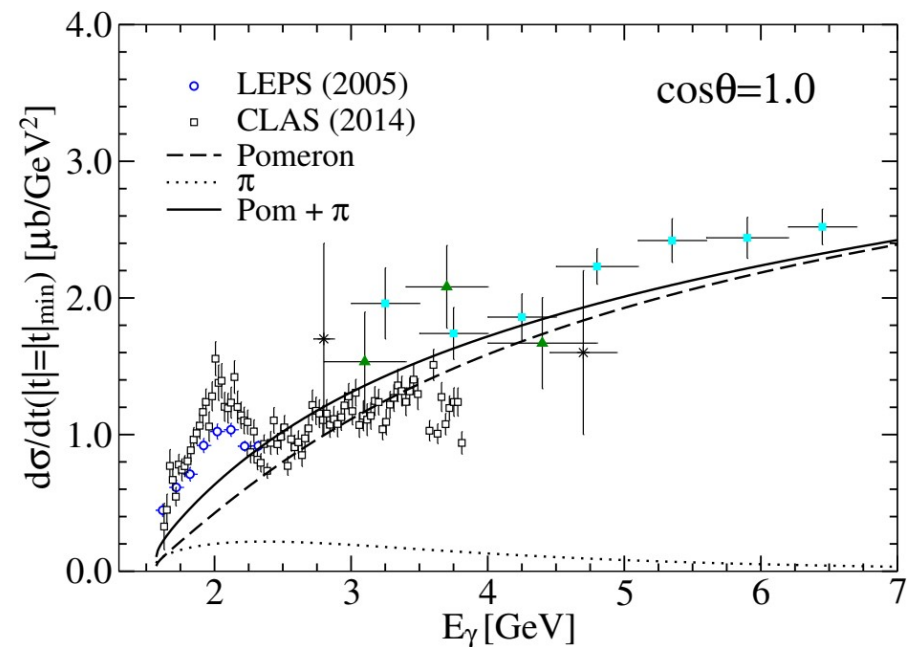
- ◇  $\varphi$  photoproduction,  $\gamma p \rightarrow \varphi(1020)p$ , is reanalyzed with effective Lagrangians .
- ◇ Abundant CLAS(2014) data are reported at full angles & low energies.
- ◇ Various contributions from t-channel exchanges and  $N^*$  exchange are considered in addition to the dominant Pomeron exchange.
  - ⇒ Odderon
  - ⇒  $f'_2(1525)$  trajectories
  - ⇒ pseudoscalar meson ( $\pi, \eta$ )
  - ⇒ scalar meson ( $a_0, f_0$ )
- ◇ Extension to other vector-meson ( $\rho, \omega$ ) photo- and electro-production mechanisms.

Thank you very much

Back Up

- Nagano, Toki, Proceedings (1998)  
: scalar glueball ( $J^{\pi}=0^{+}$ ,  $M_{gl}^2 \simeq 3 \text{ GeV}^2$ ).
- Williams, PRC, 57, 223 (1998)  
:  $s\bar{s}$  knockout, nonzero  $\varphi$ NN couplings.
- Titov et al., PRC, 60, 035205 (1999)  
: scalar mesons ( $\sigma, a_0, f_0$ ).
- Laget, PLB, 489, 313 (2000)  
:  $f_2(1270)$  meson, two gluon exchange.
- Titov, Lee, PRC, 67, 065205 (2003)  
:  $f_2(1270), f'_2(1525)$  mesons,  $N^*$ .
- ∴ Pomeron & pseudoscalar mesons ( $\pi^0, \eta$ )  
in common.

t-channel contributions are widely studied.



Mibe(LEPS)PRL.95.182001(2005)

After an observation of the bump structure, most of works have moved on to the  $N^*$  scenario.

• Titov, Kampf, PRC, 76, 035202 (2007)

: Pomeron + ( $\pi, \eta$ ) mesons.

a. Ozaki, Hosaka, Nagahiro, Scholten, PRC, 80, 035201 (2009)

: coupled-channel effective-Lagrangian method based on the K-matrix approach.

Suggest the existence of a  $N^*$ ,  $J^P=1/2^-$  resonance ( $M=2.250$ ,  $\Gamma=0.100$  [GeV]).

b. Kiswandhi, Xie, Yang, PLB, 691, 214 (2010)

: Assume a  $N^*$  resonance of  $J^P=3/2^-$  ( $M=2.10\pm 0.03$ ,  $\Gamma=0.465\pm 0.141$  [GeV]).

c. Kiswandhi, Yang, PRC, 86, 015203 (2012)

:  $N^*$  of  $J^P=3/2^\pm$  ( $M=2.08\pm 0.04$ ,  $\Gamma=0.501\pm 0.117$ (P=+),  $0.570\pm 0.159$ (P=-) [GeV]).

d. Ryu, Titov, Hosaka, Kim, PTEP, 2014, 023D03 (2014)

: various hadronic rescattering contributions, focusing on the  $K\Lambda(1520)$  channel.

